Chemical Engineering Science, Volume 308, April 2025. Article number 121357
DOI:10.1016/j.ces.2025.121357

In situ nanoconfinement catalysis for rapid hydrodechlorination of chlorophenol

Uddin Sk Raihan [a], Jingqi Zhang [b], Jingbo Chao [c], Qing Hu [d]*, Frederic Coulon [e], Xiao Jin Yang [a]*
[a] *State Key Laboratory of Chemical Resource Engineering, Beijing University of Chemical Technology, Beijing 100029, China*
[b] *Technical Centre for Soil, Agriculture and Rural Ecology and Environment, Ministry of Ecology and Environment, Beijing 100012, China*
[c] *Chemical Metrology and Analytical Science Division, National Institute of Metrology, Beijing 100029, China*
[d] *School of Environmental Science and Engineering, Southern University of Science and Technology, Shenzhen 518055, PR China*
[e] *School of Water, Energy and Environment, Cranfield University, Cranfield MK43 0AL, UK*
Corresponding authors: Qing Hu, E-mail: huq@sustech.edu.cn; Xiao Jin Yang, E-mail: yangxj@buct.edu.cn

Abstract
Chlorinated phenols are highly toxic to human and ecosystem and their biological degradation is difficult. In this work, a novel MgAlNi alloy catalyst was developed for rapid chemical degradation of p-chlorophenol (4-CP) in water under mild conditions via *in situ* hydrodechlorination (*i*HDC) without external hydrogen gas supply. A complete conversion of 0.195 mM 4-CP to phenol was achieved within 15 min with a reaction rate constant of 7.65 h^{-1}, 19.4 times higher than that of the traditional Raney Nickel (AlNi alloy) catalyst. The excellent performance of MgAlNi alloy catalyst is attributed to enhanced H_2 generation by Mg etching, surface self-reconstruction by growth of *in situ* layered double hydroxide (*i*LDH) nanosheets of 0.08-1 nm, exposed active sites of AlNi intermetallic compounds Al_3Ni_2 and Al_3Ni. The findings of this study provide new insights into broader applications of nanoconfinement catalysis to environmental remediation and open a new domain of *in situ* nanoconfinement catalysis (*i*NCC).

Keywords: Al-Ni intermetallic compounds; Chlorophenol; MgAlNi alloy; *In situ* hydrodechlorination; *In situ* nanoconfinement catalysis.

Highlight
- A novel MgAlNi catalyst is developed for in situ hydrodechlorination of chlorophenol;
- The hydrodechlorination rate by MgAlNi is 19-80 times higher than that by Raney Ni;
- In situ layered double hydroxide nanosheets are critical to Raney Ni's catalytic activity;
- A new concept of in situ nanoconfinement catalysis (iNCC) is proposed.

1. Introduction
Chlorinated phenols are emerging contaminants, which are increasingly found in the environment due to their widespread applications. Their toxic and carcinogenic properties and resistance to conventional biological treatment have been calling for robust methods to remove chlorinated phenols from water (Jiang et al. 2017, Wu et al. 2019). Chemical degradation via *in situ* hydrodechlorination (*i*HDC) has been investigated for p-chlorophenol (4-CP), a representative of chlorophenols in aqueous solutions by zero-valent metals(Xie et al. 2021) , such as zero-valent iron (ZVI) and zero-valent aluminum (ZVAl). The efficiency is relatively low because of the surface passivation of ZVI and ZVAl, rapid agglomeration of ZVI, and their poor catalytic activities (Fu et al. 2014).

These problems are greatly overcome by the use of bimetallic catalysts such as Ni/Fe (Xu et al. 2012), Pd/Fe(Wan et al. 2020), Pd/Al (Yang et al. 2013), and Pd/Mg (Patel et al. 2007), which are prepared by chemical deposition of the second catalytic metal onto the surface of the electronegative metals (Al, Mg, and Fe). The *i*HDC performance was improved by accelerating electron transfer due to numerous galvanic interactions between two metals. For instance, the reaction rate constant of 4-CP degradation by Fe/Pd bimetal was 100 times that by ZVI (Wan et al. 2020). However, such bimetals are not uniform and the catalytic effect diminishes when the second catalytic metal falls out upon the corrosion of electronegative metal (Lin et al. 2024). Bimetal alloys prepared by the melting method are relatively homogeneous and particularly, the intermetallic compounds are observed to catalyze electron transfer processes in redox reactions (Alonso et al. 2012, Bao et al. 2017, Xu et al. 2017). For example, $Al_{13}Fe_4$ was found to have a similar catalytic effect with Pd toward the selective hydrogenation of organic substances (Armbrüster et al. 2012). Raney nickel (AlNi alloy in 50% Al and 50% Ni) has been extensively investigated for hydrogenation of 2-cyclohexen-1-one (Pisarek et al. 2009), lignin (Lam et al. 2015) and polycyclic aromatic hydrocarbons, hydrodehalogenation of pesticides (Zinovyev et al. 2005), antiseptics and diclofenac (Bendová et al. 2022) and *i*HDC of chlorinated organic compounds (Wang et al. 2020). The primary limitation of Raney Nickel catalyst for *i*HDC is its reliance on a highly alkaline environment to promote aluminum-driven hydrogen

Published by Elsevier. This is the Author Accepted Manuscript issued with: Creative Commons Attribution License (CC:BY 4.0).
The final published version (version of record) is available online at DOI:10.1016/j.ces.2025.121357. Please refer to any applicable publisher terms of use.

generation and high concentrations of leached Al^{3+} ions. For example, 0.5 M KOH was used to degrade diclofenac and other biocidal contaminants (Bendová et al. 2022). Clearly, such high alkaline concentrations are not environmentally sustainable for water remediation. Therefore, improving surface reactivity of Raney Nickel and immobilizing the released Al^{3+} ions without dosing additional chemicals are of great interest.

Layered double hydroxide (LDH) is a naturally occurring clay mineral and its general molecular formula is $\left[M^{II}_{1-x}M^{III}_{x}OH_2\right]^{x+}(A^{n-})_{x/n} \cdot mH_2O$, where M^{II} and M^{III} are divalent and trivalent metal cations and A^{n-} is an anion in the interlayer space(Wang et al. 2012, Forano et al. 2013, Yu et al. 2019, Chen et al. 2024). LDH's solubility constant is in a range of 10^{-40}-10^{-50} and LDH has been extensively employed for super-mineralization of heavy metal ions and Al^{3+} (Liu et al. 2011, Qian et al. 2012). LDH nanomaterials have long been employed as catalysts for pollutant degradation (Chen et al. 2024), H_2 generation (Yan et al. 2016) and CO_2 reduction (Bi et al. 2022, Jerome et al. 2022) and the catalytic enhancement of LDH nanomaterials is ascribed to a so-called nanoconfinement catalysis (NCC), which has been well acknowledged to increase reaction rates and improve the selectivity of chemical synthesis (Fu et al. 2019, Grommet et al. 2020). Considering the unique, thermodynamically stable layered structure of LDH, the nanoconfinement effect of LDH nanomaterial can be further augmented by *in situ* generation of LDH nanosheets because the dynamics of divalent and trivalent metal ion crystallization into LDH could significantly improve electron transfer. The challenge is a constant supply of Mg^{2+} and Al^{3+} with molar ratios of 2-4 in a constant pH 10 medium. In previous publications, we developed novel MgAl alloys for removing complex mixtures of heavy metals and organic pollutants (Zhang et al. 2022). Zerovalent Al and Mg in the alloy provide electrons for transformation of pollutants and generation of hydrogen gas while the released Mg^{2+} and Al^{3+} react in situ to produce LDH nanosheets on the surface of the alloy. Therefore, we consider that the catalytic activity of Raney Nickel (AlNi alloy) for iHDC of 4-CP in water can be improved by alloying Raney Ni with Mg via *in situ* nanoconfinement catalysis (iNCC). The aim of this study is to systematically investigate Raney Nickel, MgAl and MgAlNi alloys, Mg metal, and mixtures of Mg, Al and Ni metals to prove the new concept of *in situ* nanoconfinement catalysis (iNCC).

2. Experimental

2.1. Chemicals and materials

Analytical grade chemicals, unless otherwise specified, were used throughout the study. P-chlorophenol, $CuCl_2$, HCl (99.7%) and NaOH (99.7%), EDTA, methanol (high-performance liquid chromatography grade) were purchased from Beijing Chemicals, China. Mg (>99.9%), Al (>99.9%) and Ni (>99.9%) metal powders (>200 mesh) were purchased from Tianjin Guangfu Fine Chemical Research Institute (China). Raney Ni (AlNi alloy, Al and Ni in 50%/50 % by weight, 325 meshes, 45 μm) was purchased from Tianjin Shield Specialty Chemical Ltd Co., China). MgAl alloy (50%/50% by weight) was provided by Tangshan Weihao Magnesium Powder Co., Ltd, Qianan, Hebei, China, Raney Nickel (AlNi alloy, 50/50,) was obtained from Aladdin reagent (Shanghai) Co., Ltd. MgAlNi alloys were prepared by melting pure Mg (>99.9%), Al (>99.9%) and Ni (>99.9%) ingots (mass ratio 25:25:50) using MgO crucible in a vacuum electric furnace (SGM.VB6/16, Sigma Furnace Industry, China) at a vacuum pressure of <5 Pa. The temperature of the furnace was increased from room temperature to 1300 °C at a rate of 7 °C/min and was maintained for 30 min. The furnace was then cooled to room temperature and the MgAlNi alloy ingot was crushed into powders and sieved.

2.2. Reductive degradation reaction

The degradation experiments were carried out in a flask with 200 mL, a catalyst concentration of 2.5 g/L (unless otherwise specified), 0.195 mM 4-CP under magnetic stirring (500 rpm) and room temperature (25°C ± 3°C) conditions. Aliquot samples (3 mL) were extracted and filtered at predetermined intervals with a 0.22 μm organic nylon membrane. The residual amount of 4-CP, the phenol concentration, the pH value, and the metal ion concentration in the solution were measured later. After the experiment, the solution's residual alloy was washed, filtered, and vacuum-dried (30°C) for 12 h for characterization analysis. The experiment was carried out in triplicate to obtain accurate data, and their mean value was used in this research. The impact of pH on HDC was investigated by modifying the pH of the solution from 2 to 11 with 0.1 M HCl and NaOH. Additionally, various operational parameters were subjected to comprehensive examination, including catalyst concentration, particle size, and the synergistic effect of other contaminants.

The degradation efficiency is calculated using $\frac{C}{C_0} \times 100\%$, where C and C_0 are the corresponding concentration at a certain reaction time and the initial concentration of 4-CP, respectively. Experimental errors

are calculated by relative percent difference RPD = $\frac{C_1 - C_2}{(C_1 + C_2)/2} \times 100\%$, where C_1 = larger of the observed values and C_2 = smaller of the observed values (Asgari et al. 2024).

2.3. Analysis and characterization methods

Quantitative analysis of the parent and daughter compounds (4-CP and phenol) was performed with high-performance liquid chromatography (HPLC) on a Thermo Fisher Ultimate 3000 HPLC system (Thermo, Ultimate 3000, U.S.A.) equipped with a reversed-phase ZORBAX Eclipse XDB-C18 column (5.0 mm×250 mm, 5 µm) and the diode array detector. The mobile phase was methanol and deionized water, with a ratio of 70:30 (v:v). The flow rate was set at 1 mL/min, and the column oven temperature was 30°C. The injection volume for all samples was 10 µL and was analyzed at the wavelength of 280 nm. The alloy catalyst used in this research was characterized by X-ray diffraction (XRD) and scanning electron microscopy (SEM) before and after the batch experiment respectively. XRD was performed on a D8 Advance (Bruker, Germany) using Cu Kα radiation with a scanning range from 10° to 90°. The surface morphology of the alloy was analyzed by SEM (Hitachi, S-4700, Japan). The concentration of dissolved metal ions in aqueous samples such as Al, Mg, Ni, and Cu was detected by inductively coupled plasma-optical emission spectrometry (ICP-OES, Thermo, iCAP 6000, U.S.A.) to analyze the corrosion of the alloy catalyst during the reaction. A pH meter (Mettler Toledo, FE 20, China) determined the pH value of the solution.

3. Results and discussion

3.1 Effect of catalyst composition and structure

The *i*HDC performance of different catalysts for 4-CP in water is shown in Fig. 1. Clearly, MgAl and Raney Ni alloys, Mg metal, and mixtures of Al, Mg and Ni metals are not effective whereas MgAlNi alloy is able to transform 4-CP to phenol at an initial pH of 5.8. The concentration of 4-CP is reduced by greater than 50% in 2 h by MgAlNi alloy and phenol concentration increase is well matched with the decrease of 4-CP concentration (the mass balance is within ± 34.6%) (Fig. 1a). The 4-CP concentration variation as a function of reaction time follows the first order reaction and the rate constant is 0.44 h^{-1}. The pH increases sharply to 11.1 in 15 min and then decreases slowly to 10.6 by 120 min. Interestingly, a similar trend with pH is observed for the concentration of Mg^{2+}, which reaches a peak of 9.08 mM at 15 min, indicating a possible mechanism that Mg provides electrons to dissociate H_2O to H_2 while releasing OH^- (Fig. 1b). Catalyst composition is a critical factor for hydrodechlorination of chlorophenol (Ma et al. 2020, Hegedüs et al. 2021), while the above results demonstrate that there are structural and/or other factors in the MgAlNi alloy to promote the iHDC of 4-CP in aqueous solution.

Ni catalysts including Raney Ni have been extensively investigated for hydrodechlorination of chlorophenol by external H_2 supply and *in situ* H_2 generation from the hydrolysis of active metal of the catalysts (Table 1). Phenol is the end product of the hydrodechlorination of chlorophenol and HCl is the byproduct regardless of the catalysts(Ma et al. 2015). The byproduct HCl has been considered to poison and deactivate the catalysts and adding inorganic and organic alkalis (e.g., NaOH, KOH, Na_2CO_3, Triethylamine) can eliminate the poisoning effect of HCl (Ma et al. 2020). Liquid-phase iHDC is likely more applicable to water remediation because external H_2 supply suffers safety risk and high cost in the transportation and storage of H_2 gas. However, high concentrations of alkalis are generally required in order to produce sufficient H_2 for iHDC. On the other hand, alkaline treatment dissolves part of Al from Raney Ni alloy producing porous three dimensional, increasing the porosity and specific surface area and exposing active sites (Lei et al. 2001, Zinovyev et al. 2007), but also causing secondary contamination by leaching of Al and Ni (Colin et al. 1992). The alkaline treatment may also causes a collapse of the structure and skeleton of Raney Ni alloy's intermetallic compounds (Al_3Ni_2, Al_3Ni) while Al oxides and hydroxides on the surface are likely to deactivate the Raney Ni catalyst (Lei et al. 2001). The results in Fig. 1 and Table 1 indicate that alloying MgAlNi alloy significantly improve the catalytic activity of Raney Ni at mild conditions.

Table 1. Hydrodechlorination of 4- chlorophenol in aqueous solution by different catalysts

Catalyst	Dosage (g/L)	pH	4-CP conc. (mM)	Time (h)	Removal (%)	Rate constant (h^{-1})	References
Ni-Fe	6	2-8	0.21	1	99.3	--	(Xu et al. 2012)
Pd/PPy-rGO/foam-Ni, **	Pd, 0.43 mg / cm^3	3-5.1	0.78	2	95.3	--	(Yu et al. 2020)
Fe^0 / Cu^0, Raney Ni	3	3-10	0.31	1	100	6.54	(Raut et al. 2020)
Raney Ni*	0.24	6.85 mM NaOH	6.2	0.5	100	3.06	(Ma et al. 2015)
Raney Ni	1.6	0.5 M KOH	0.2	0.83	89	2.1	(Bendová et al. 2022)
Raney Ni	2.5	2	0.195	2	37.5	0.394	Current work
MgAlNi	2.5	2	0.195	0.25	99	7.65	Current work
Catalyst	Dosage (g/L)	pH	4-CP conc. (mM)	Time (h)	Removal (%)	Rate constant (h^{-1})	References
Ni-Fe	6	2-8	0.21	1	99.3	--	(Xu et al. 2012)
Pd/PPy-rGO/foam-Ni, **	Pd, 0.43 mg / cm^3	3-5.1	0.78	2	95.3	--	(Yu et al. 2020)
Fe^0 / Cu^0, Raney Ni	3	3-10	0.31	1	100	6.54	(Raut et al. 2020)
Raney Ni*	0.24	6.85 mM NaOH	6.2	0.5	100	3.06	(Ma et al. 2015)
Raney Ni	1.6	0.5 M KOH	0.2	0.83	89	2.1	(Bendová et al. 2022)
Raney Ni	2.5	2	0.195	2	37.5	0.394	Current work
MgAlNi	2.5	2	0.195	0.25	99	7.65	Current work

* External H_2 supply at a flowrate of 10 mL/min; ** Electrolysis H_2 production

3.2 Effect of initial pH

Not only does the pH affect the production of active hydrogen but also the formation of metal oxides and hydroxides and the surface reactivity/passivation of metal catalysts. The effect of initial pH on 4-CP's degradation by MgAlNi and AlNi alloys is shown in Fig. 2 a, b. The removal rate by MgAlNi increases with decreasing initial pH of the solution. In stark contrast, the rate is significantly enhanced at pH 2.0 with a removal rate of 99.9% in 15 min and a rate constant of 7.65 h^{-1}, 19.4-80.5 times higher than that at initial pH 5.8-9.0 (Fig. 2 a) and the rate is not significantly affected by pH in the Raney Nickel catalytic system (Fig. 2 b). The increase of phenol concentration matches the decrease of 4-CP in the MgAlNi alloy system (Fig. 2 c) and the pH is all lifted to 10.5-11.4 in 15 min and then remains almost constant in the following period of 105 min (Fig. 2d). Clearly, the catalytic activity of AlNi alloy is significantly improved by alloying with Mg.

3.3 Degradation mechanism

In general, the surface of Raney Ni alloy is deactivated by Al oxides and can be reactivated by pretreatment with acids and alkalis at ambient temperature and hydrogen gas reduction at high temperature (Fouilloux 1983) Nevertheless, the surface is prone to re-deactivate after acid pretreatment due to the increase of pH when the acid is neutralized by hydroxide ions released from the hydrolysis of Al metal. The distinct advantage of MgAlNi alloy over Raney Ni alloy is that the pH remains almost constant at 10.5-11.4 after 15 min reaction at initial pH 2-9. pH 10-11 is considered as the optimal condition of Raney Ni's catalysis while the accelerated dissolution of Mg from the alloy at initial pH 2 provides sufficient H_2 and exposes active sites of the catalyst. Clearly, the constant pH around 11, sufficient H_2 and enhanced exposure of the catalyst active sites are important factors for rapid hydrodechlorination of 4-CP. Nevertheless, we consider that the in situ generation of MgAl-LDH nanosheets on the surface of the catalyst plays a critical role in the rapid iHDC of 4-CP. Not only does the in situ generation of LDH (iLDH) nanosheets maintain a constant pH of 11 by incorporating OH- into the LDH molecules but also create numerous nanoconfinement spaces. Most recently, we achieved rapid and efficient reduction of Cr(VI) in a wide pH range of 3-11 by MgAlFe alloy and proposed that in situ LDH nanosheets play a critical role (Chen et al. 2024). Similarly, the in situ LDH nanosheets could prevent the aggregation of Ni atoms and Al-Ni intermetallic compounds and maintain a well-dispersion of these phases of new nanomaterials when the MgAlNi alloy is eroded. Therefore, a conceptual illustration of in situ nanoconfinement catalysis (iNCC) is proposed in Fig. 3 for rapid iHDC of 4-CP by MgAlNi alloy.

The surface of MgAlNi alloy is relatively smooth before 4-CP degradation (Fig. 4 a) and transformed to a flower-like structure (Fig. 4 b), which is a typical morphology of LDH. The XRD analyses indicate that the

pristine alloy consists of $Mg_{17}Al_{12}$, Al_3Ni_2, Mg_2Ni, and Mg_6Ni (Fig. 4 c). Leaching of Mg and Al atoms exposes active sites of the catalyst and creates defects of the intermetallic compounds and numerous interfaces by the in situ formation of LDH nanosheets. The resultant product consists of three phases $Mg_3Al_2(OH)_{18}$•$4.5H_2O$ with 69.59% crystallinity, $Mg_{0.833}Al_2(OH)_{0.176}(CO_3)_{0.083}H_2O_{0.75}$ with 70.10% crystallinity) and $Mg(OH)_2$ with 72.75% crystallinity. By contrast, no significant changes are observed before and after 4-CP degradation for both composition and surface morphology of Raney Ni catalyst (Fig. 4 d, e, f).

3.4 Effect of particle size and dosage

The specific surface area is important to the catalyst activity (Cheng et al. 2007). In this study, three different particle sizes of 10-20, 20-40 and 200-300 meshes are examined (Fig. 5 a), which shows that a reaction time of 18, 10 and 0.5 h is required to achieve greater than 99.9% removal for 0.195 mM 4-CP, respectively. MgAlNi alloy dosage (2.5, 5, 10 and 20 g/L removes 10.87%, 36.92%, 53.10% and 94.56%, respectively within 2 h (Fig. 5b).

3.5 Effect of Cu and EDTA

Both transition metals and EDTA are increasingly found in various water bodies and therefore, the effects of Cu^{2+}, a representative transition metals and EDTA, a common ingredient of agrochemicals, are investigated. The results are shown in Fig. 6. Both Cu^{2+} and EDTA promote the removal of 4-CP by MgAlNi alloy (Fig. 6 a, b) whereas they do not make a significant improvement when Raney Ni is employed as the catalyst (Fig. 6 c, d). Cu^{2+} has been observed to catalyze the reductive transformation of nitrate by AlFe alloys (Hou et al. 2015, Zhang et al. 2019) and nanoscale zero valent Al (Zhao et al. 2014)or Fe (Khalil et al. 2016) while being reduced to metallic Cu, which deposits on the surface of the alloy and creates numerous galvanic microcells, thus enhancing the electron transfer rate between the pollutants and the active metal of the alloy. The concentrations of Mg^{2+}, Al^{3+}, Ni^{2+} and Cu^{2+} at initial pH 2 and 5.8 are given in Table 2. Cu^{2+} concentration is reduced to 0.25 mg/L from addition of 300 mg/L and Ni^{2+} concentration is below 0.05 mg/ L in the MgAlNi alloy system. This indicates that the integrity of Ni atoms is well maintained. However, a considerably high concentration of Ni^{2+} is found in the case of 10 mM EDTA, indicating that the addition of EDTA causes the dissolution of Ni atoms out of the alloy. It is also noted that high concentrations of Ni^{2+} (9-10 mg/L) and Al^{3+} (24-88 mg/L) are found in the Raney Ni catalyst system. This demonstrates the superiority of MgAlNi alloy over Raney Ni in water remediation.

Critical resource recovery from water is becoming a new and promising strategy for water remediation (Kazi et al. 2023) while waste utilization is critical to circular economic development (Foroutan et al. 2020). For example, desalination brine was employed to modify clay catalyst for advanced oxidation processes (AOP) to degrade azithromycin in water (Mojahedimotlagh et al. 2024). It was reasonably anticipated that the spent catalyst of MgAlNi alloy after the treatment of complex water would eventually turn to LDH, which may contain small amounts of residual Mg, Al, Ni, intermetallic compounds and divalent and trivalent transition metals which were originally present. These types of LDH could be directly used or modified as catalysts in AOP for wastewater treatment.

Table 2.

Metal ions concentration leached from MgAlNi and AlNi alloys in different conditions.

	$Al_{50}Ni_{50}$				$MgAlNi_{50}$			
pH_0	2.0	5.8	5.8*	5.8**	2.0	5.8	5.8*	5.8**
Al^{3+}	30.51	23.98	87.76	30.82	0.09	0.13	0.41	0.25
Mg^{2+}	-	-	-	-	33.60	6.47	49.23	91.97
Ni^{2+}	10.54	8.94	10.90	20.03	0.02	<0.02	0.04	6.59
Cu^{2+}	-	-	2.77	-	-	-	0.25	-

*Addition of 300 mg/L Cu(II); **Addition of 10 mM EDTA

4. Conclusion

A novel MgAlNi alloy in a composition of 25%, 25% and 50% by weight has been developed for in situ hydrodechlorination of chlorophenol in water under mild conditions and is superior to conventional Raney Ni catalyst regarding the hydrodechlorination rate in pH 2-9, secondary contamination by leached Al^{3+} and Ni^{2+} and simultaneous removal of heavy metals. Specifically, the hydrodechlorination of 0.195 mM 4-chlorophenol at initial pH 2 is completed in 15 min by MgAlNi alloy catalyst and the rate constant is 19.4

times higher than that by Raney Ni alloy while the leaching of Al and Ni is 339 and 527 times respectively lower. The excellent catalytic performance of MgAlNi alloy is attributed to a synergistic effect by in situ MgAl-LDH nanosheets and Mg-Al-Ni intermetallic compounds in unique hierarchical micro-nanostructures and the findings and results support a new concept of in situ nanoconfinement catalysis (iNCC). Further investigation is warranted for the effect of MgAlNi alloy's composition and long-term catalytic activity.

Credit authorship contribution statement: Uddin Sk Raihan: Investigation, Methodology, Data curation, Writing - original draft. Jingqi Zhang: Visualization, Validation, Methodology. Jingbo Chao: Writing - review & editing. Frederic Coulon: Writing - review & editing. Qing Hu: Writing - review & editing. Xiao Jin Yang: Conceptualization, Funding acquisition, Supervision, Writing - review & editing, Methodology.

Competing Interests: The authors declare that they have no known competing financial interests or personal relationships that could have appeared to influence the work reported in this paper.
Corresponding author: Qing Hu and Xiao Jin Yang
Funding: Not applicable.
Ethical Approval: Not applicable.
Consent to participate: Not applicable.
Consent for publication: Not applicable.
Data availability: All data generated or analyzed during this study are included in this published article.

References

1. Alonso, D. M., S. G. Wettstein and J. A. Dumesic (2012). "Bimetallic catalysts for upgrading of biomass to fuels and chemicals." Chemical Society Reviews **41**(24): 8075-8098.

2. Armbrüster, M., K. Kovnir, M. Friedrich, D. Teschner, G. Wowsnick, M. Hahne, P. Gille, L. Szentmiklósi, M. Feuerbacher and M. J. N. M. Heggen (2012). "Al13Fe4 as a low-cost alternative for palladium in heterogeneous hydrogenation." **11**(8): 690-693.

3. Asgari, G., A. Seid-Mohammadi, A. Rahmani, R. Shokoohi and H. J. J. o. M. L. Abdipour (2024). "Concurrent elimination of arsenic and nitrate from aqueous environments through a novel nanocomposite: Fe3O4-ZIF8@ eggshell membrane matrix." **411**: 125810.

4. Bao, Z., Q. Hu, W. Qi, Y. Tang, W. Wang, P. Wan, J. Chao and X. J. J. J. o. e. m. Yang (2017). "Nitrate reduction in water by aluminum alloys particles." **196**: 666-673.

5. Bendová, H., B. Kamenická, T. Weidlich, L. Beneš, M. Vlček, P. Lacina and P. Švec (2022). "Application of Raney Al-Ni alloy for simple hydrodehalogenation of Diclofenac and other halogenated biocidal contaminants in alkaline aqueous solution under ambient conditions." Materials **15**(11): 3939.

6. Bi, Z.-x., R.-t. Guo, X. Hu, J. Wang, X. Chen and W.-g. J. N. Pan (2022). "Research progress on photocatalytic reduction of CO 2 based on LDH materials." **14**(9): 3367-3386.

7. Chen, Y., J. Tan, J. Chao, J. Zhang, Y. Tang, Y. Liu, Q. Hu, F. Coulon, X. J. J. A. A. M. Yang and Interfaces (2024). "In situ nanoconfinement catalysis for highly efficient redox transformation." **16**(45): 62010-62021.

8. Cheng, R., J.-l. Wang and W.-x. Zhang (2007). "Comparison of reductive dechlorination of p-chlorophenol using Fe0 and nanosized Fe0." Journal of hazardous materials **144**(1-2): 334-339.

9. Colin, P., S. Hamar-Thibault and J. J. J. o. m. s. Joud (1992). "Metallurgical structure and alkali leaching of the Al/Al 3 Ni eutectic." **27**: 2326-2334.

10. Forano, C., U. Costantino, V. Prévot and C. T. Gueho (2013). Chapter 14.1 - Layered Double Hydroxides (LDH). Developments in Clay Science. F. Bergaya and G. Lagaly, Elsevier. **5:** 745-782.

11. Foroutan, R., S. J. Peighambardoust, R. Mohammadi, M. Omidvar, G. A. Sorial and B. J. I. j. o. b. m. Ramavandi (2020). "Influence of chitosan and magnetic iron nanoparticles on chromium adsorption behavior of natural clay: adaptive neuro-fuzzy inference modeling." **151**: 355-365.

12. Fouilloux, P. (1983). "The nature of raney nickel, its adsorbed hydrogen and its catalytic activity for hydrogenation reactions (review)." Applied Catalysis **8**(1): 1-42.

13. Fu, F., D. D. Dionysiou and H. Liu (2014). "The use of zero-valent iron for groundwater remediation and wastewater treatment: a review." Journal of hazardous materials **267**: 194-205.

14. Fu, Q. and X. J. N. C. Bao (2019). "Confined microenvironment for catalysis control." **2**(10): 834-836.

15. Grommet, A. B., M. Feller and R. Klajn (2020). "Chemical reactivity under nanoconfinement." Nature nanotechnology **15**(4): 256-271.

16. Hegedüs, M., K. Gáborová, T. Weidlich, P. Kalivoda, J. Briančin and E. J. J. o. E. C. E. Tóthová (2021). "Rapid hydrodehalogenation of chlorinated benzoic acids using mechano-thermally prepared Raney alloy with enhanced kinetics." **9**(4): 105764.

17. Hou, M., Y. Tang, J. Xu, Y. Pu, A. Lin, L. Zhang, J. Xiong, X. J. Yang and P. J. J. o. E. C. E. Wan (2015). "Nitrate reduction in water by aluminum–iron alloy particles catalyzed by copper." **3**(4): 2401-2407.

18. Jerome, M. P., F. A. Alahmad, M. T. Salem and M. J. J. o. E. C. E. Tahir (2022). "Layered double hydroxide (LDH) nanomaterials with engineering aspects for photocatalytic CO2 conversion to energy efficient fuels: Fundamentals, recent advances, and challenges." **10**(5): 108151.

19. Jiang, G., M. Lan, Z. Zhang, X. Lv, Z. Lou, X. Xu, F. Dong, S. J. E. s. Zhang and technology (2017). "Identification of active hydrogen species on palladium nanoparticles for an enhanced electrocatalytic hydrodechlorination of 2, 4-dichlorophenol in water." **51**(13): 7599-7605.

20. Kazi, O. A., W. Chen, J. G. Eatman, F. Gao, Y. Liu, Y. Wang, Z. Xia and S. B. J. A. M. Darling (2023). "Material design strategies for recovery of critical resources from water." **35**(36): 2300913.

21. Khalil, A. M., O. Eljamal, S. Jribi and N. J. C. E. J. Matsunaga (2016). "Promoting nitrate reduction kinetics by nanoscale zero valent iron in water via copper salt addition." **287**: 367-380.

22. Lam, C. H., C. B. Lowe, Z. Li, K. N. Longe, J. T. Rayburn, M. A. Caldwell, C. E. Houdek, J. B. Maguire, C. M. Saffron and D. J. J. G. C. Miller (2015). "Electrocatalytic upgrading of model lignin monomers with earth abundant metal electrodes." **17**(1): 601-609.

23. Lei, H., Z. Song, D. Tan, X. Bao, X. Mu, B. Zong and E. J. A. C. A. G. Min (2001). "Preparation of novel Raney-Ni catalysts and characterization by XRD, SEM and XPS." **214**(1): 69-76.

24. Lin, H., Y. Liu, J. Deng, L. Jing, Z. Wang, L. Wei, Z. Wei, Z. Hou, J. Tao and H. Dai (2024). "Bimetallic nanoparticles: advances in fundamental investigations and catalytic applications." Environmental Science: Advances.

25. Liu, Q., Y. Li, J. Zhang, Y. Chi, X. Ruan, J. Liu and G. Qian (2011). "Effective removal of zinc from aqueous solution by hydrocalumite." Chemical Engineering Journal **175**: 33-38.

26. Ma, X., S. Liu, Y. Liu, X. Li, Q. Li, G. Gu and C. Xia (2020). "Promoted liquid-phase hydrodechlorination of chlorophenol over Raney Ni via controlling base: Performance, mechanism, and application." Chemosphere **242**: 125202.

27. Ma, X., Y. Liu, X. Li, J. Xu, G. Gu and C. Xia (2015). "Water: the most effective solvent for liquid-phase hydrodechlorination of chlorophenols over Raney Ni catalyst." Applied Catalysis B: Environmental **165**: 351-359.

28. Mojahedimotlagh, F., E. A. Nasab, R. Foroutan, D. Ranjbar Vakilabadi, S. Dobaradaran, E. Azamateslamtalab and B. Ramavandi (2024). "Azithromycin decomposition from simple and complex waters by H2O2 activation over a recyclable catalyst of clay modified with nanofiltration process brine." Environmental Technology & Innovation **33**: 103512.

29. Patel, U. D. and S. Suresh (2007). "Dechlorination of chlorophenols using magnesium–palladium bimetallic system." Journal of hazardous materials **147**(1-2): 431-438.

30. Pisarek, M., M. Łukaszewski, P. Winiarek, P. Kędzierzawski and M. Janik-Czachor (2009). "Selective catalytic hydrogenation of isophorone on Ni–Al alloy modified with Cr." Materials Chemistry and Physics **114**(2): 774-779.

31. Qian, G., L. Feng, J. Z. Zhou, Y. Xu, J. Liu, J. Zhang and Z. P. Xu (2012). "Solubility product (Ksp)-controlled removal of chromate and phosphate by hydrocalumite." Chemical Engineering Journal **181-182**: 251-258.

32. Raut, S. S., R. Shetty, N. M. Raju, S. P. Kamble and P. S. Kulkarni (2020). "Screening of zero valent mono/bimetallic catalysts and recommendation of Raney Ni (without reducing agent) for dechlorination of 4-chlorophenol." Chemosphere **250**: 126298.

33. Wan, H., M. S. Islam, N. J. Briot, M. Schnobrich, L. Pacholik, L. Ormsbee and D. Bhattacharyya (2020). "Pd/Fe nanoparticle integrated PMAA-PVDF membranes for chloro-organic remediation from synthetic and site groundwater." Journal of membrane science **594**: 117454.

34. Wang, Q. and D. O'Hare (2012). "Recent Advances in the Synthesis and Application of Layered Double Hydroxide (LDH) Nanosheets." Chemical Reviews **112**(7): 4124-4155.

35. Wang, W., J. Niu and Z. J. J. o. h. m. Yang (2020). "An efficient reduction of unsaturated bonds and halogen-containing groups by nascent hydrogen over Raney Ni catalyst." **389**: 121912.

36. Wu, S., K. Tang, J. Zhang, X. Chen, H. Hu, Q. Hu, X. J. J. W. S. Yang and Technology (2019). "Removal of 4-chlorophenol from polluted water by aluminum–iron alloys." **80**(6): 1099-1106.

37. Xie, J., C. Lei, W. Chen, Q. Xie, Q. Guo and B. Huang (2021). "Catalytic properties of transition metals modified nanoscale zero-valent iron for simultaneous removal of 4-chlorophenol and Cr(VI): Efficacy, descriptor and reductive mechanisms." Journal of Hazardous Materials **403**: 123827.

38. Xu, F., S. Deng, J. Xu, W. Zhang, M. Wu, B. Wang, J. Huang and G. Yu (2012). "Highly Active and Stable Ni–Fe Bimetal Prepared by Ball Milling for Catalytic Hydrodechlorination of 4-Chlorophenol." Environmental Science & Technology **46**(8): 4576-4582.

39. Xu, J., Y. Pu, W.-K. Qi, X. J. Yang, Y. Tang, P. Wan and A. Fisher (2017). "Chemical removal of nitrate from water by aluminum-iron alloys." Chemosphere **166**: 197-202.

40. Yan, K., G. Wu and W. J. E. T. Jin (2016). "Recent advances in the synthesis of layered, double-hydroxide-Based materials and their applications in hydrogen and oxygen evolution." **4**(3): 354-368.

41. Yang, B., Y. Zhang, S. Deng, G. Yu, Y. Lu, J. Wu, J. Xiao, G. Chen, X. Cheng and L. J. C. e. j. Shi (2013). "Reductive degradation of chlorinated organic pollutants-contaminated water by bimetallic Pd/Al nanoparticles: effect of acidic condition and surfactants." **234**: 346-353.

42. Yu, H., S. Yang, B. Zhao, Y. Lu, S. Zhu, X. Wang, W. Qin and M. Huo (2020). "Enhanced electrochemical dechlorination of 4-chlorophenol on a nickel foam electrode modified with palladium, polypyrrole and graphene." Journal of Electroanalytical Chemistry **869**: 114099.

43. Yu, W., H. Li, N. Du, W. J. J. o. c. Hou and i. science (2019). "Estimation of surface free energy and solubility parameters of MgAl layered double hydroxides." **546**: 361-370.

44. Zhang, J., H. Hu, J. Chao, Y. Tang, P. Wan, Q. Yuan, A. C. Fisher, F. Coulon, Q. Hu and X. J. Yang (2022). "Groundwater remediation using Magnesium–Aluminum alloys and in situ layered doubled hydroxides." Environmental Research **204**: 112241.

45. Zhang, J., J. Wu, J. Chao, N. Shi, H. Li, Q. Hu and X. J. Yang (2019). "Simultaneous removal of nitrate, copper and hexavalent chromium from water by aluminum-iron alloy particles." Journal of contaminant hydrology **227**: 103541.

46. Zhao, W., X. Zhu, Y. Wang, Z. Ai and D. J. C. E. J. Zhao (2014). "Catalytic reduction of aqueous nitrates by metal supported catalysts on Al particles." **254**: 410-417.

47. Zinovyev, S. and P. J. A. C. B. E. Tundo (2007). "On the promoting effect by quaternary ammonium salts in the multiphase hydrodechlorination with hydrogen gas on Raney nickel catalyst." **75**(1-2): 124-128.

48. Zinovyev, S. S., N. A. Shinkova, A. Perosa and P. J. A. C. B. E. Tundo (2005). "Phase-transfer promotion of hydrodechlorination of chlorophenoxy-pesticides over Pd/C and Raney-Ni." **55**(1): 49-56.

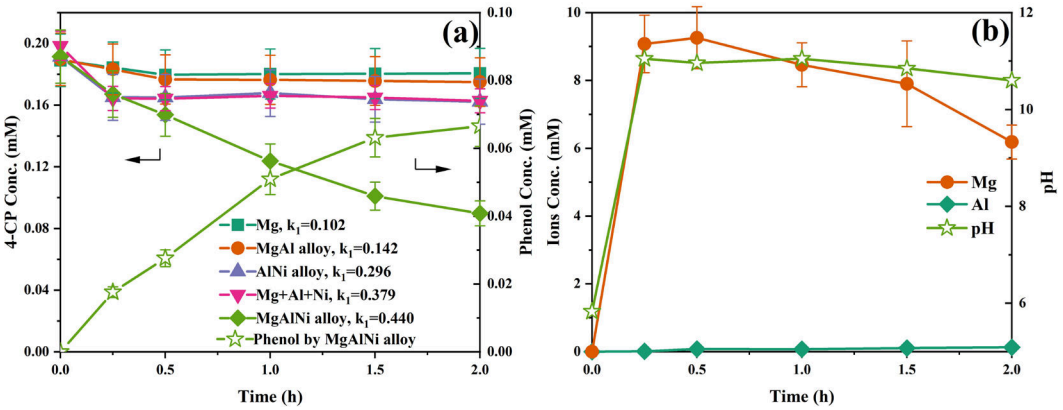


Fig. 1. Effect of different catalytic systems - Mg metal, MgAl, AlNi and MgAlNi alloys, and mixtures of Mg, Al and Ni metal powders (Mg+Al+Ni). (a) Concentrations of 4-CP and phenol, (b) pH and concentrations of Mg2+ and Al3+ as a function of reaction time. Solution volume 200 mL; initial 4-CP concentration 0.195 mM; initial pH=5.8; catalyst loading 2.5 g/L; catalyst particle size 200-300 mesh; temperature 25 ± 0.5°C.

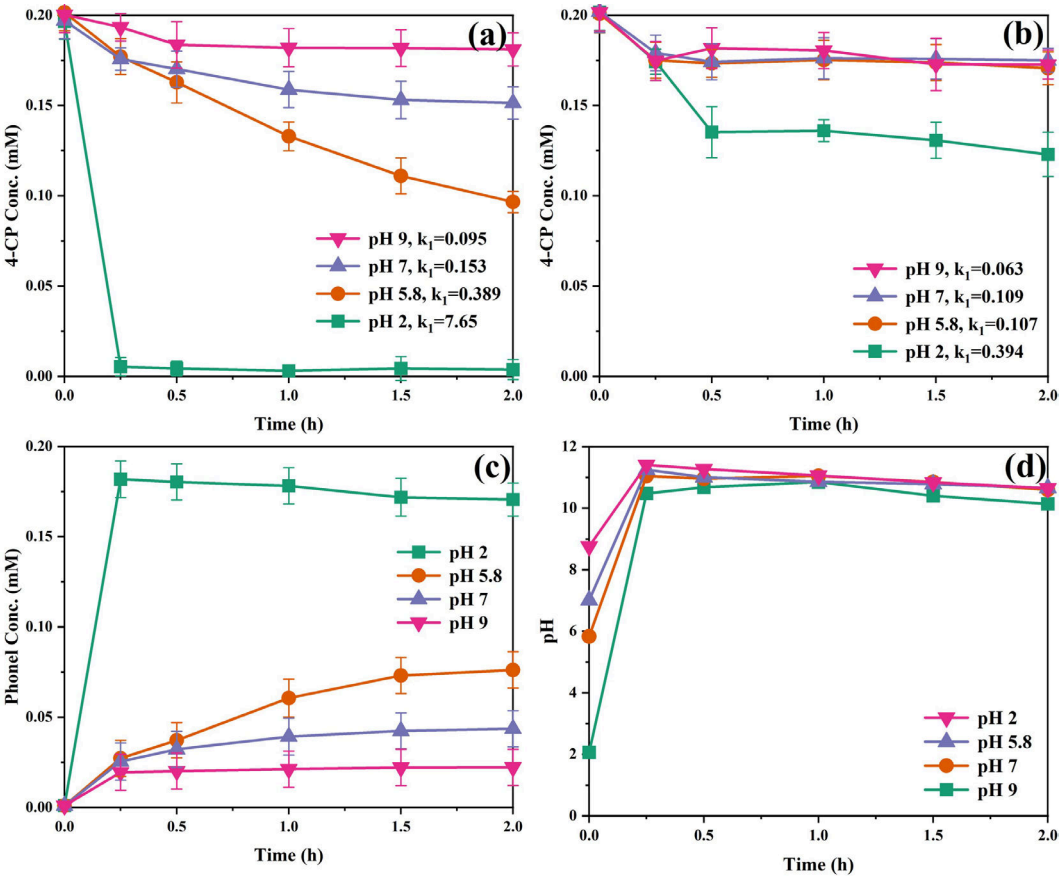


Fig. 2. Effect of initial pH on degradation of 4-CP by (a) 4-CP concentration by MgAlNi alloy, (b) 4-CP concentration by AlNi alloy, (c) phenol concentration by MgAlNi alloy, (d) pH by MgAlNi alloy. Solution volume 200 mL; initial 4-CP concentration 0.195 mM; catalyst loading 2.5 g/L; catalyst particle size 200-300 mesh; temperature 25 ± 0.5°C.

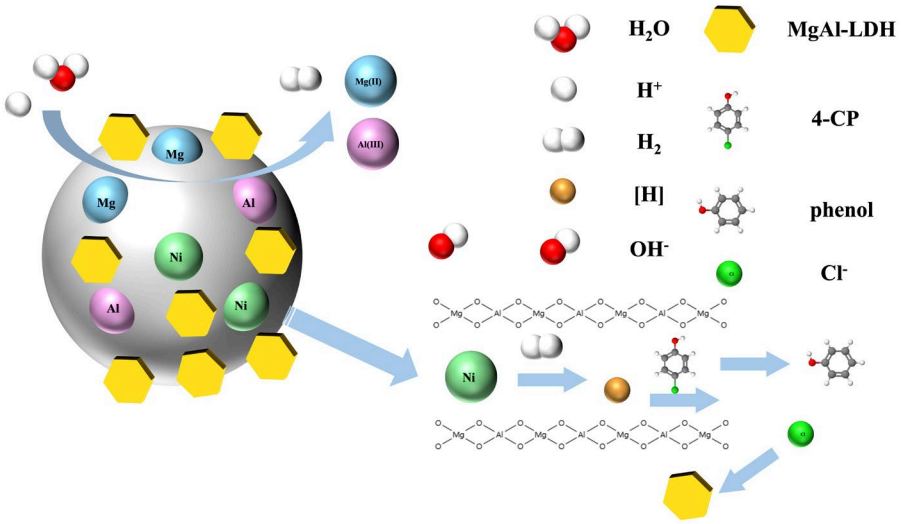


Fig. 3. A schematic illustration of in situ nanoconfinement catalysis (iNCC) by MgAlNi alloy for rapid hydrodechlorination of 4-chlorophenol in water.

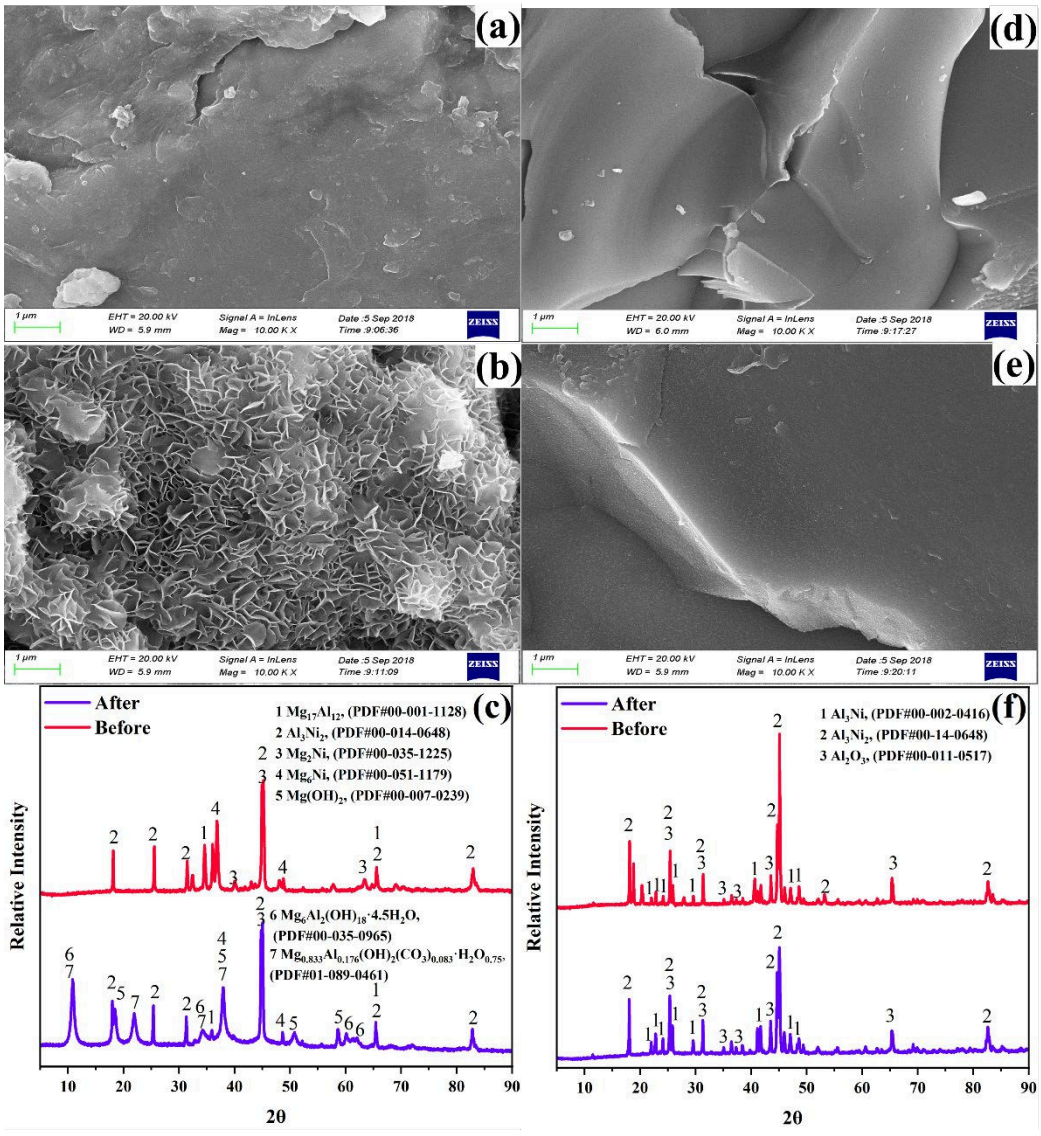


Fig. 4. SEM and XRD characterization of the catalysts before and after 4-CP's hydrodechlorination reaction. (a) MgAlNi alloy before the reaction, (b) MgAlNi alloy after the reaction, (c) MgAlNi alloy before the reaction, (d-f) AlNi alloy.

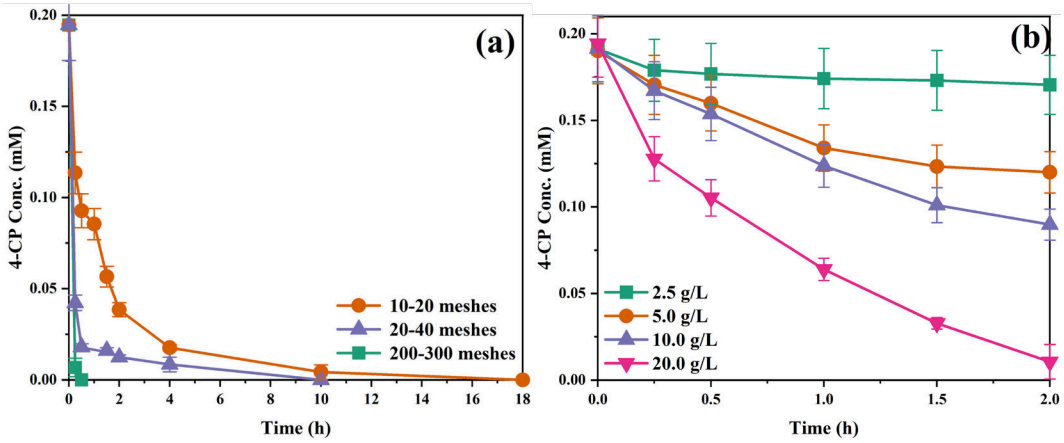


Fig. 5. The effect of MgAlNi alloy catalyst particle size (a) with particle sizes of 200-300 meshes; (b) in a catalyst loading of 2.5 g/L and dosage . Solution volume 200 mL; initial 4-CP concentration 0.195; initial pH=5.8; temperature 25 ± 0.5°C.

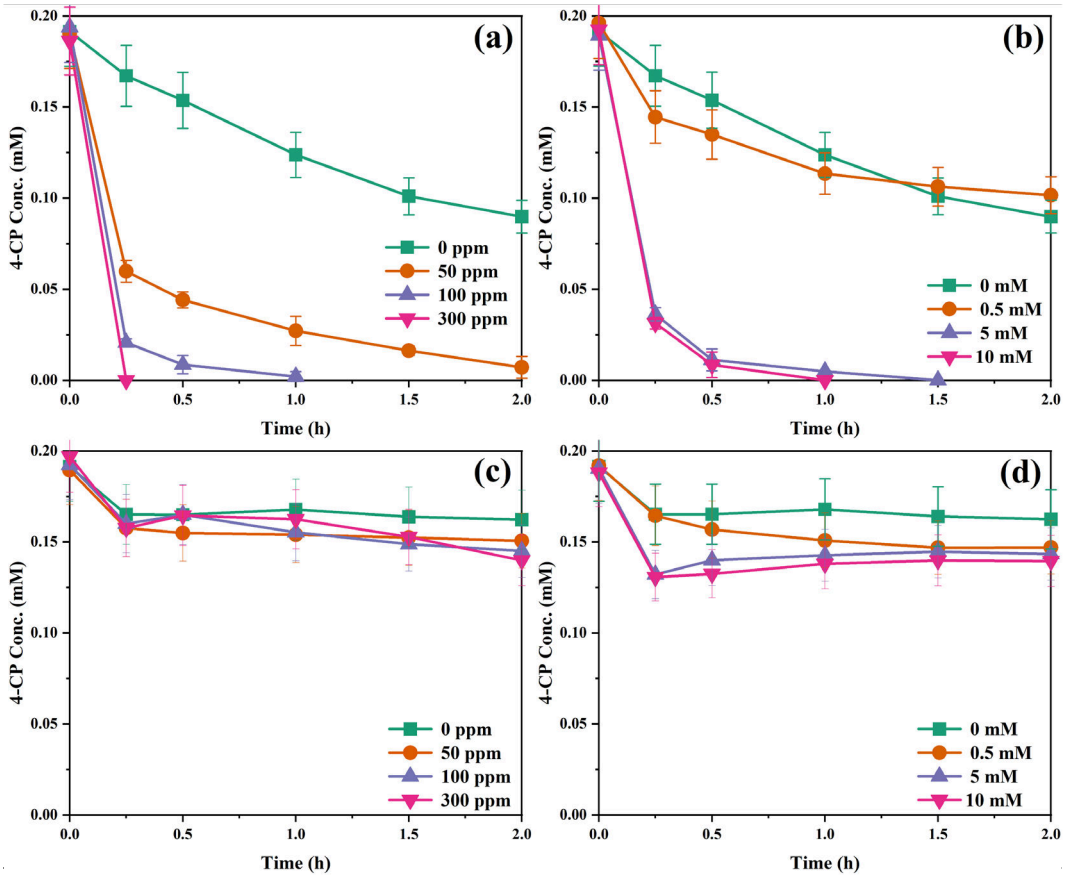


Fig. 6. Effect of the concentrations of $CuCl_2$ and EDTA on 4-CP degradation. (a) MgAlNi alloy with $CuCl_2$, (b) MgAlNi alloy with EDTA, (c) Raney Ni alloy with $CuCl_2$, (d) Raney Ni alloy with EDTA. Solution volume 200 mL; initial 4-CP concentration 0.195 mM; initial pH=5.8; catalyst particle size 200-300 mesh; catalyst loading 2.5 g/L; temperature 25 ± 0.5°C.



https://dspace.org/

In situ nanoconfinement catalysis for rapid hydrodechlorination of chlorophenol

Raihan, Uddin Sk; Zhang, Jingqi; Chao, Jingbo; Hu, Qing; Coulon, Frederic ...

2025-04-01
Elsevier
https://doi.org/10.1016/j.ces.2025.121357
Raihan US, Zhang J, Chao J, et al., (2025) In situ nanoconfinement catalysis for rapid hydrodechlorination of chlorophenol. Chemical Engineering Science, Volume 308, April 2025. Article number 121357

Downloaded from a DSpace repository. https://dspace.org/